A Novel Approach to Selection of Dopant to Immobilize Neodymium in Uranium-Based Metallic Fuels

Rabi Khanal[a,], Nathan Jerred[a,b,c], Michael T. Benson[c], D.A. Andersson[d], Robert D. Mariani[c], Indrajit Charit[a], Samrat Choudhury[a,]

[a] *Department of Chemical and Materials Engineering, University of Idaho Moscow, ID 83844, USA*
[b] *Center for Advanced Energy Studies, Idaho Falls, ID, 83401, USA*
[c] *Idaho National Laboratory, PO Box 1625, Idaho Falls, ID, 83415*
[d] *Los Alamos National Laboratory, Los Alamos, NM, 87545, USA*

Abstract

Formation of intermetallic compounds of lanthanide fission products within uranium-based metallic fuels with added dopant(s) has been proposed to arrest fission products within the metallic-matrix, before lanthanides chemically react with cladding materials, leading to degradation of the cladding. Unlike previous *trial-and-error* approach, here we present *ab-initio* based generic alloy-design principles to identify dopant(s) for a given lanthanide to form dopant-lanthanide intermetallic. Our approach correctly identifies previously known dopant like Pd, as well as predict novel dopants (As and Se) which can bind fission product Nd within U-matrix. Formation of our predicted NdAs intermetallic within the U-matrix has been confirmed experimentally.

Keywords: Metallic fuel, FCCI, Fuel additive, First-principle calculations

Design of alloy composition often has competing objectives depending on the application of alloys. While in the case of high-entropy alloys (HEAs) formation of intermetallic compounds is typically avoided [1], intermetallic precipitates of lanthanides fission products and dopants are desired in metallic fuel for fast reactors [2]. In the latter case, a formation of such intermetallic helps to arrest lanthanides within the metallic matrix, before lanthanides chemically react with cladding materials, leading to degradation of the cladding [2, 3, 4, 5]. However, appropriate choice of dopants to immobilize fission products is a non-trivial task

Email address: `samrat@uidaho.edu` (Samrat Choudhury)

as a range of fission products are known to form (e.g., fuel after 8 % burnup was found to compose of 1.17% of Nd, 0.71 % of Ce, 0.35 % of Pr and other elements [2]). Further, one or more dopants may be required to arrest individual lanthanide fission product [6]. Choosing appropriate dopant(s) for targeted precipitation is a challenging task for materials scientist in general and not limited to U-based fuel.

Previous attempts to choose potential dopants based on lanthanide-dopant binary phase diagrams, and macroscopically measured thermodynamic properties (e.g., melting point) [3, 2] had limited success in arresting lanthanides (Ln), plausibly due to the lack of understanding of chemical and electronic interaction between elements as well as lack of comprehensive list of U-Ln-dopant ternary phase diagrams. Alternatively, *ab-initio* calculations can be adapted to predict novel dopants as they provide fundamental understanding regarding the electronic structure and chemical interactions between elements, without particular need for their binary and ternary phase diagrams [7]. In this work, we present a combined *ab-initio* calculation and experimental approach on screening dopants to immobilize Nd, the primary lanthanide fission product. We show that dopants can be screened based on readily available features such as electronic configuration, electronegativity, and covalent radius of dopants. Our approach correctly identifies previously known dopants like Pd [8, 9], as well as predict novel dopants (As and Se) which can bind with fission product Nd within the U-matrix.

All the calculations were performed using the Vienna *Ab initio* Simulation Package (VASP) [10] with the Perdew-Burke-Ernzerhof (PBE) functional [11] within projected augmented plane wave method [12]. The internal atomic positions were optimized with a HellmanFeynman force convergence threshold of 0.05 eV/Å. A cut off energy of 450 eV and $6 \times 3 \times 3$ Monkhorst Pack grid were used during optimization. The system was modeled as follows: a U atom was substituted with a Nd atom on fully optimized $3 \times 3 \times 3$ supercell of α-U, *Cmcm* (orthorhombic) structure. Within the positions optimized Nd-U system a U atom at the first nearest neighbor position to the Nd atom was substituted with the dopant (X) and the atomic positions were re-optimized.

The enthalpy of mixing of different dopants in Nd-U system was calculated as follows

[13]:

$$\Delta E_{\mathrm{mixing}} = E(\mathrm{U}_{m-2}\mathrm{NdX}) + E(\mathrm{U}) - E(\mathrm{U}_{m-1}\mathrm{Nd}) - E(\mathrm{X}), \quad (1)$$

in which $E(\mathrm{U}_{m-2}\mathrm{NdX})$ is the total energy of $(m-2)$U atoms, and one atom of Nd and dopant (X) in a simulation cell of m sites; $E(\mathrm{U}_{m-1}\mathrm{Nd})$ is the total energy of $(m-1)$U atoms and one Nd in a simulation cell of m sites. E(X) and E(U) are the total energy per atom for X and U, respectively. In our scheme, negative enthalpy indicates attractive interaction between elements, implying ease of formation of the stable compounds [1, 14]. We later arc melt cast two U-Nd-As alloys with different weight %, namely alloy1 (92U-4Nd-4As) and alloy2 (94U-4Nd-2As). Alloy1 and alloy2 has Nd:As an atomic ratio of 1:2 and 1:1, respectively. The alloys were later characterized by scanning electron microscopy (SEM), energy dispersive x-ray spectroscopy (EDS) and X-ray diffraction (XRD), in order to verify the formation of Nd-As compound(s) as tendency of which was predicted by our *ab-initio* calculations. More details on computational and experimental methods are presented in Supplemental Information.

To understand the linkage between dopants electronic structure and its inherent tendency to form Nd-dopant intermetallic compound, we inspect the valence electronic configurations of previously successful dopant like Pd (nd^{10}), and Sb (np^3), and unsuccessful elements like Tl (np^1) to form intermetallic with Nd. Based on our initial inspection, we hypothesized that dopants with relatively more stable electronic configurations (half-filled and filled orbitals), should exhibit a higher tendency to form an intermetallic compound with Nd compared to dopants with partially filled orbitals. Further, commonly used empirical Hume-Rothery rules [15] implies that the propensity to form dopant-Nd intermetallic compound increases with the increase in the difference of electronegativity and covalent radius between dopant and Nd. To test our hypothesis on relative compound forming tendency, we calculated the enthalpy of mixing for several possible dopants as a function of electronegativity (Figure 1(a)) and covalent radius (Figure 1(b)) of the dopants. Dopants were selected based on electronic configuration (e.g., As, (np^3), half-filled orbitals), and their electronegativity and covalent radius. For reference, Nd has a covalent radius of 201 pm and electronegativity of

1.14 on the Pauling scale [16]. It is notable that, dopant As and Se (np^4) were never tried before as a potential dopant.

Overall, in Figure 1, we found that mixing enthalpy decreases and increases with the increase in electronegativity and covalent radius of the dopants, respectively. The large negative values of mixing enthalpy of As and Se suggest the strong tendency to form stable compounds with Nd. Dopants such as Sb, Te, Ga, and Pd expected to exhibit intermediate tendency, while Tl is the least favorable in forming a stable compound with Nd. Our prediction is in agreement with the previous findings, where Tl was found to be the least effective [4], and Sb [4, 17] and Pd [8, 9] were more effective in immobilizing lanthanides. Further, to understand the nature of chemical interactions between the dopant and Nd, we plotted the charge density difference (CDD) at each atomic position between the Nd-U-X and Nd-U structures. Two distinct trends were observed in CDD. Strongly electronegative dopants such as As, Se and Pd exhibit strong ionic interaction with a significant amount of charge transferred (shown by yellow isosurface) from Nd to the dopant compared to less electronegative dopants such as In, and Tl (Figure 1(c-h)). Our Bader charge analysis also provide secondary evidence of such charge transfer (see Supplemental Information).

To gain a further understanding of the electronic interactions between Nd and dopants, we have plotted partial DOS of dopant and Nd in Nd-U-X systems as shown in Fig. 2(a)-(f). Similar to CDD, the partial DOS plots also show two distinct patterns. Unlike the case for Ga, In and Tl, Figure 2(d)-(f) shows that localized Nd $4f$ orbitals (located between -5 to -4 eV) interacts with dopants via valence electrons, namely, p electrons in As, Se, and d electrons in Pd (shown by shaded region, Figure 2(a)-(c)). This overlap of orbitals indicates possible orbitals hybridization between Nd and dopants As, Se, and Pd. Such orbital hybridization resulted in a significant sharing of charge between Nd and the dopant As, Se and Pd atoms (Figure 2)(g)-(i). Given the position of overlap in the energy with respect to the Fermi level, this interaction is not expected to be very strong. However, this may act as another factor for the binding between Nd and dopants As, Se and Pd in addition to the strong ionic interaction caused by electronegativity difference. Combined covalent and strong ionic interactions between dopants As, Se and Pd with Nd, may facilitates the

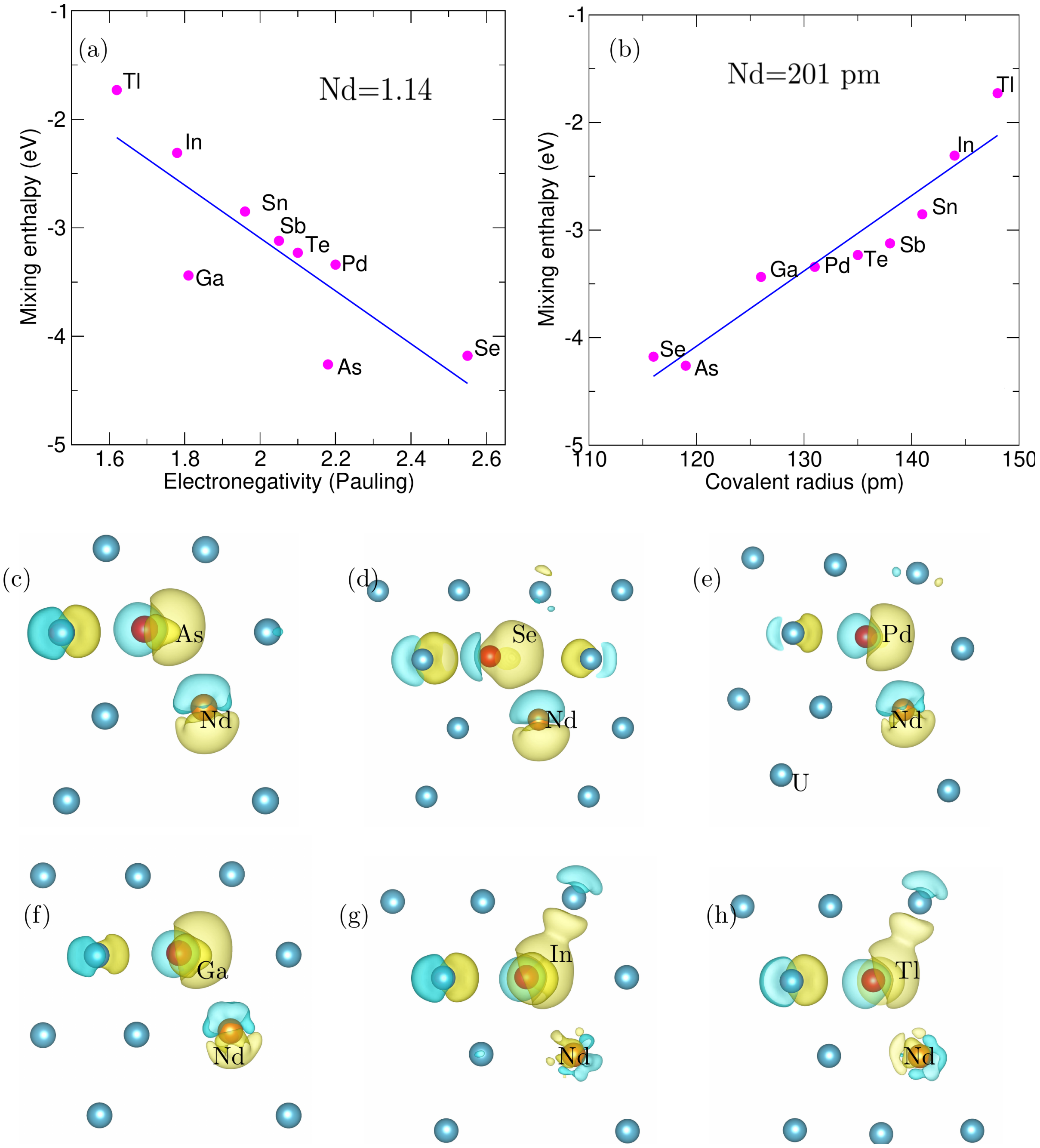

Figure 1: (a) The correlation between mixing enthalpy and the electronegativity of dopant. (b) The correlation between mixing enthalpy and covalent radius of dopant. The electronegativity and the covalent radius are from the Ref. [16]. (c)-(h) The charge density difference (CDD) between Nd-U-X and Nd-U systems; Nd gives charge to dopants for their binding. The yellow isosurface represents excess charge, and blue isosurface represents charge deficit.

formation of dopant-Nd intermetallic compounds.

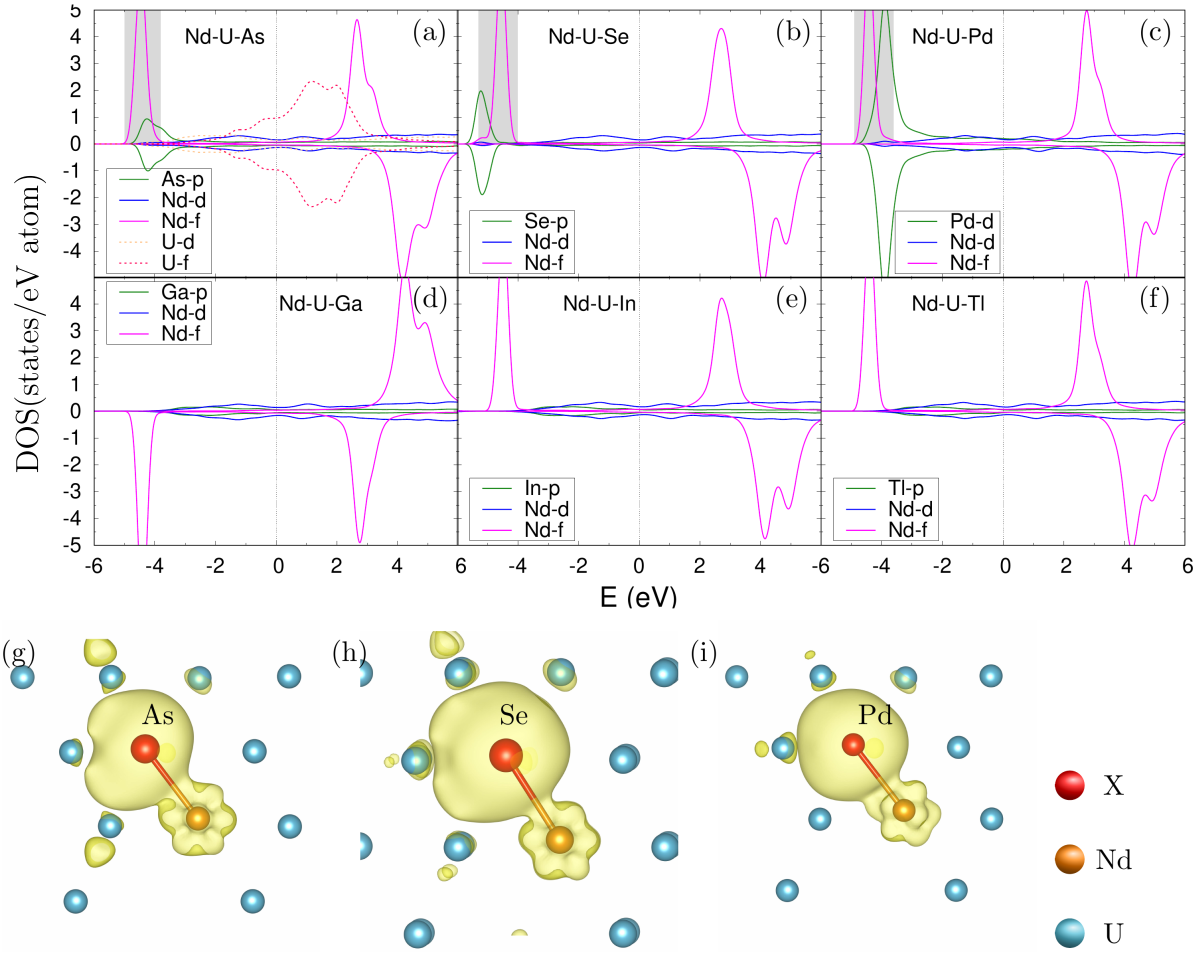

Figure 2: Orbital resolved DOS for Nd-U-X systems, where X=As (a), Se (b), Pd (c), Ga (d), In (e), or Tl (f). The vertical dashed line represents the Fermi level. The states in negative and positive vertical axis represent down and up spin components, respectively. U-DOS remain more or less similar in all systems, The charge density plotted for the slice of energy that includes overlap between Nd $4f$ orbital with p orbitals for As (g), Se (h) and d orbitals for Pd (i). Color code, red = dopants(X), golden = Nd, cyan = U and the yellow represents the isosurface of charge.

Another interesting observation is that all dopants that exhibit less tendency in forming stable compounds with Nd, the outermost orbitals always have less than the half-filled of maximum number of electrons, i.e., np^1 (In and Tl) and np^2 (Sn). It follows that the elements that have a relatively more stable electronic configuration filled or half-filled compared to the partially filled appear to be more effective in tendency of forming a stable compound with Nd with Se (np^4) as an exception. However, Se has strong difference in electronegativity and covalent radius with Nd. We conclude that the intrinsic tendency of a dopant to form intermetallic compound with Nd is governed by three factors (a) difference in dopant-Nd electronegativity; (b) difference in dopant-Nd covalent radius and (c) dopants electronic configuration. Among the dopants Tl least satisfies these criteria and is expected to exhibit least tendency to form intermetallic compounds with Nd, which has been confirmed previously [4]. On the contrary As (np^3, half-filled orbitals) satisfies all the three criteria exhibit highest negative enthalpy of mixing and hence should be able to form intermetallic compound with Nd which we will experimentally verify in the next section. In the case of Ga in the Pauling scale has an electronegativity of 1.81, which is close to the value for In (1.81) and Sn (1.96). However, the smaller covalent radius of Ga (np^1) compared to In (144 pm), and Sn (141 pm) may have resulted in highly negative enthalpy of mixing. This implies there could be competition between the effects of covalent radius versus electronegativity on the enthalpy of mixing. The modern machine learning tools, such as principal component analysis [18], may help to determine the relative importance of individual factors.

Overall, the uniqueness of our alloy design criteria listed above is its simplicity. The tendency of a dopant to form intermetallic within a metallic matrix can be predicted simply based on readily available elemental features without creating complicated binary and ternary phase diagrams. Our work emphasizes the need to understand electronic configurations of elements for effective alloy design, a criterion not explicitly included within Hume-Rothery rules or Darken-Gurry map [19]. Further, based on the enthalpy of mixing, our work provides a quantitative estimate of the tendency of dopant to form intermetallic with Nd. This is unlike the Hume-Rothery rule or Darken-Gurry map, which only provides a qualitative estimate for the dopant-Nd intermetallic compound formation tendency.

In-reactor condition, fission product Nd is continuously generated within the U-matrix. In order to verify the formation of *ab-initio* predicted Nd-As intermetallic and its stability within the U-matrix, we cast two alloys. Alloy1, representing initial stages of the formation of fission products when the externally added concentration of dopant As is higher than Nd (Nd:As atomic ratio of 1:2) and alloy2 with equal atomic ratio of As to Nd (Nd:As atomic ratio of 1:1) representing later stage of the formation of fission product. Backscattered electron SEM images (Figure 3(a-b)) of these U-Nd-As alloys reveals the formation of two precipitated phases within the matrix, dark-grey and light-grey precipitates. The precipitated phases are observed to be evenly distributed throughout the microstructure and range in size between 5 to 20 μm. EDS point chemical analysis was conducted on several precipitates of interest in both the alloys; selected points are shown in Figure 3(a-b); the corresponding compositions of each analysis point are listed in Table 1. The dark-grey precipitates are found to be consisted of Nd and As at roughly a 1:1 atomic ratio; indicating that they are likely the NdAs phase. The light-grey precipitates consisting of U and As and are observed to bind at an atomic ratio of roughly 3:4 (or possibly 1:1), which would correspond to the U_3As_4 (or UAs) phase. Based on our *ab-initio* calculated negative enthalpy of mixing for As in the α-U matrix is $\approx$ -1eV, as compared to greater negative mixing enthalpy of As in Nd-U matrix (-4.26 eV), it is intuitive that in alloy1 any excess As remains after binding with Nd may form compound with U matrix. For the same reason no U-As compound is observed in alloy2, which has a lower As content than Nd, Table 1. Overall, the presence of the NdAs precipitates in both these alloys indicate its formation is more favorable within the U matrix. Based on the results of mixing enthalpy and the experimental observations in both alloy1 and alloy2, we suggest that for in-reactor applications, U-based alloys should have excess As compared to the expected Nd generated at maximum burnup. From thermodynamic consideration it is expected that as Nd is continuously generated within the matrix, As would be released from the U and bind with Nd, as seen from the preference of As for Nd over U from our calculated enthalpy of mixing of As in U and Nd-U matrix. Finally, it should be pointed out that NdAs, U_3As_4, and UAs phases are stable, equilibrium phases as found in their corresponding binary phase diagrams [20, 21].

For accurate identification of the phases formed in these U-Nd-As alloys (Figure 3(c and d)) XRD was performed. Beside confirming the EDS point chemical analysis predicted formation of NdAs phase, diffraction data confirms that the U-As precipitates observed in the alloy1 sample are actually comprised of the UAs phase (1:1 atomic ratio) with peaks indexed at of 2θ angles of 30.8° and 44.0°. In analyzing the diffraction pattern of the

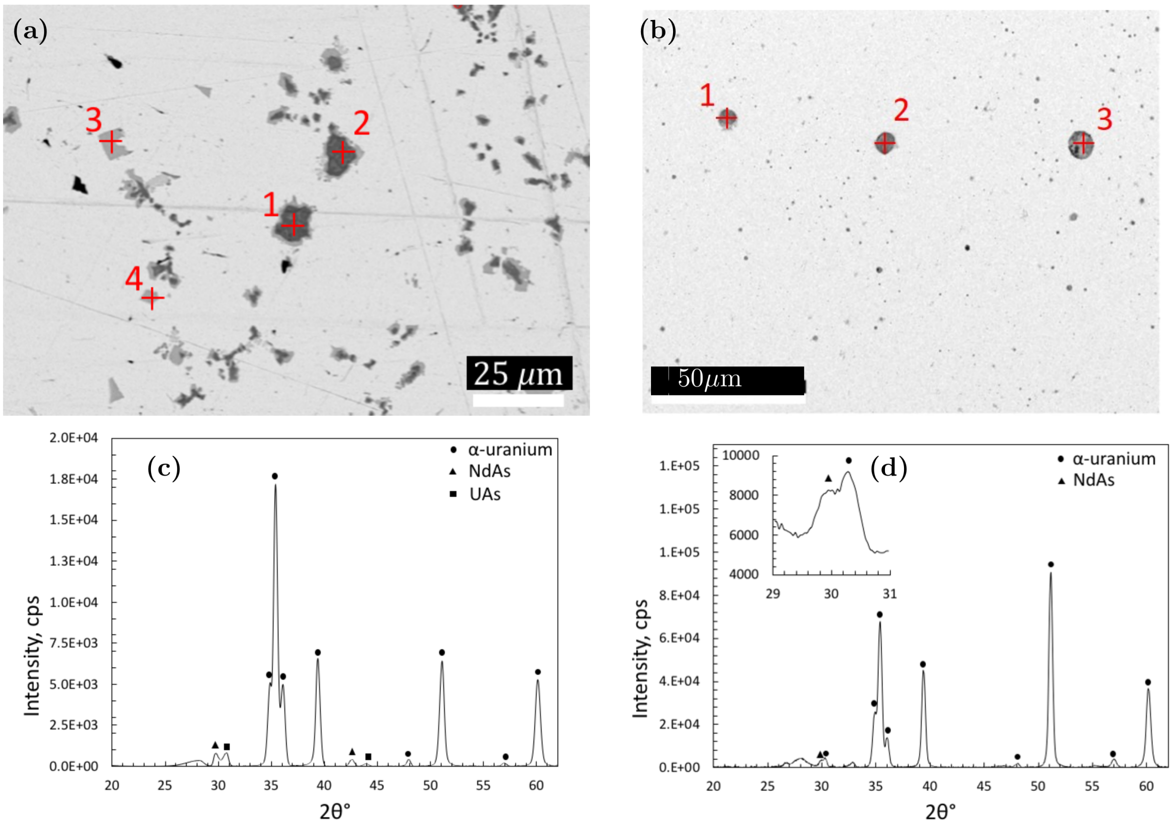

Figure 3: Backscattered electron SEM image indicating locations of EDS point analysis (a) alloy1 (92U-4Nd-4As, wt.%) (b) alloy2 (94U-4Nd-2As, wt.%). XRD patterns of (c) alloy1 and (d) alloy2 samples.

Table 1: EDS point analysis compositions of precipitates (atom %) in reference to Fig. 3 (a) alloy1 (92U-4Nd-4As, wt.%) and (b) alloy2 (94U-4Nd-2As, wt.%).

Alloys	Pt #	Precipitate	U	Nd	As	Suggested Phase
alloy1	1	dark grey	4	45	50	NdAs
	2	dark grey	5	45	50	NdAs
	3	light grey	43	2	55	UAs
	4	light grey	44	1	55	U_3As_4 or UAs
alloy2	1	dark grey	4	52	45	NdAs
	2	dark grey	0	57	43	NdAs
	3	dark grey	1	59	40	NdAs

alloy2, a peak is identified for the NdAs phase at the 2θ angles of 29.8° which is better observed in the inset of Fig. 3(d). Due to their proximity, the NdAs peak could not to be completely deconvoluted from the α-U peak, which is at 30.3°; nevertheless, its existence can still be discerned. Overall, the formation of NdAs intermetallic compound in both these alloys is further verified by our elemental EDS mapping as presented in the Supplementary Information. It should be pointed out that SEM image of alloy2 (Figure 3(b) also indicates numerous sub-micron sized round precipitates. Our elemental EDS maps of Nd and As reveal that these sub-micron precipitates have only high concentration of Nd and no As. Given our *ab-initio* calculated positive enthalpy of mixing (4.26 eV) of Nd in U, no Nd-U phase is expected to form. However, higher resolution analysis techniques would be necessary to infer the elemental compositions of such precipitates accurately.

In this study, using *ab-initio* calculations, we have developed simple alloy design principles primarily based on electronic configurations, electronegativities and covalent radius of elements involved. These principles were used to demonstrate the tendency of externally added dopants to form intermetallic within a metallic matrix in a more comprehensive manner than typically used thermodynamic approaches such as Hume-Rothery rules or Darken-Gurry map. The uniqueness of our guiding principles is that they are based on readily available elemental features without creating complicated binary/ternary phase-diagrams, as previously needed. We showed that our proposed principles are successful in correctly identifying previously known effective dopants such as Pd, Sb and less effective ones such as Tl to form intermetallic within the U-matrix. Also, guided by the same principles we identified two highly effective novel dopants, namely, As and Se as potential dopants and experimentally verified the compound forming tendency of Nd with As inside the U-matrix.

Acknowledgements

The work is being supported by the U.S. Dept. of Energy's Nuclear Energy University Programs (NEUP) under contract DE-NE0008557. This research made use of the resources of the High Performance Computing Center at Idaho National Laboratory, which is supported by the Office of Nuclear Energy of the U.S. Department of Energy and the Nuclear

Science User Facilities under Contract No. DE-AC07-05ID14517.

Data availability

The raw/processed data required to reproduce these findings cannot be shared at this time due to technical or time limitations.

[1] S. Singh, N. Wanderka, B. S. Murty, U. Glatzel, J. Banhart, Decomposition in multi-component AlCoCrCuFeNi high-entropy alloy, Acta Mater. 59 (1) (2011) 182–190. doi:10.1016/j.actamat.2010.09.023.

[2] R. D. Mariani, D. L. Porter, T. P. O'Holleran, S. L. Hayes, J. R. Kennedy, Lanthanides in metallic nuclear fuels: Their behavior and methods for their control, J. Nucl. Mater. 419 (1) (2011) 263–271. doi:10.1016/j.jnucmat.2011.08.036.

[3] Y. S. Kim, G. L. Hofman, A. M. Yacout, Migration of minor actinides and lanthanides in fast reactor metallic fuel, J. Nucl. Mater. 392 (2) (2009) 164–170. doi:10.1016/j.jnucmat.2009.03.043.

[4] G. Bozzolo, G. L. Hofman, A. M. Yacout, H. O. Mosca, Lanthanides migration and immobilization in U–Zr nuclear fuels, J. Nucl. Mater. 425 (1) (2012) 188–192. doi:10.1016/j.jnucmat.2011.05.013.

[5] N. Jerred, R. Khanal, M. Benson, E. Perez, J. King, M. Dubey, J. Burns, I. Charit, S. Choudhury, R. Mariani, Evaluation of tellurium as a fuel additive in neodymium-containing U-Zr metallic fuel, scientific reports (In Press).

[6] M. T. Benson, Y. Xie, J. A. King, K. R. Tolman, R. D. Mariani, I. Charit, J. Zhang, M. P. Short, S. Choudhury, R. Khanal, N. Jerred, Characterization of U-10Zr-2Sn-2Sb and U-10Zr-2Sn-2Sb-4Ln to assess Sn+Sb as a mixed additive system to bind lanthanides, J. Nucl. Mater. 510 (2018) 210–218. doi:10.1016/j.jnucmat.2018.08.017.

[7] G. C. Kaphle, S. Ganguly, R. Banerjee, R. Banerjee, R. Khanal, C. M. Adhikari, N. P. Adhikari, A. Mookerjee, A study of magnetism in disordered PtMn, PdMn and NiMn alloys: an augmented space recursion approach, J. Phys.: Condens. Matter 24 (29) (2012) 295501. doi:10.1088/0953-8984/24/29/295501.

[8] G. W. Egeland, R. D. Mariani, T. Hartmann, D. L. Porter, S. L. Hayes, J. R. Kennedy, Reduction of FCCI effects in lanthanide–iron diffusion couples by doping with palladium, J. Nucl. Mater. 440 (1) (2013) 178–192. doi:10.1016/j.jnucmat.2013.04.060.

[9] M. T. Benson, L. He, J. A. King, R. D. Mariani, Microstructural characterization of annealed U-12Zr-4Pd and U-12Zr-4Pd-5Ln: Investigating Pd as a metallic fuel additive, J. Nucl. Mater. 502 (2018) 106–112. doi:10.1016/j.jnucmat.2018.02.012.

[10] G. Kresse, J. Furthmüller, Efficiency of ab-initio total energy calculations for metals and semiconductors using a plane-wave basis set, Comput. Mater. Sci 6 (1) (1996) 15–50. doi:10.1016/0927-0256(96)00008-0.

[11] J. P. Perdew, K. Burke, M. Ernzerhof, Generalized Gradient Approximation Made Simple [Phys. Rev. Lett. 77, 3865 (1996)], Phys. Rev. Lett. 78 (7) (1997) 1396–1396. doi:10.1103/PhysRevLett.78.1396.

[12] G. Kresse, D. Joubert, From ultrasoft pseudopotentials to the projector augmented-wave method, Phys. Rev. B 59 (3) (1999) 1758–1775. doi:10.1103/PhysRevB.59.1758.

[13] A. E. Shields, S. E. Ruiz Hernandez, N. H. de Leeuw, Theoretical analysis of uranium-doped thorium dioxide: Introduction of a thoria force field with explicit polarization, AIP Adv. 5 (8) (2015) 087118. doi:10.1063/1.4928438.

[14] M. C. Gao, J.-W. Yeh, P. K. Liaw, Y. Zhang (Eds.), High-Entropy Alloys, Springer International Publishing, Cham, 2016. doi:10.1007/978-3-319-27013-5.

[15] W. Hume-Rothery, B. R. Coles, Atomic Theory for Students of Metallurgy., 5th Edition, no. 3 in Monograph and report series, Institute of Metals, 1969.

[16] Web elements periodic table covalent radius periodicity (2017 (Accessed: 2017-10-26)).
URL `https://www.webelements.com/periodicity/covalent-radius/`

[17] Y. Xie, M. T. Benson, J. A. King, R. D. Mariani, J. Zhang, Characterization of U-Zr fuel with alloying additive Sb for immobilizing fission product lanthanides, J. Nucl. Mater. 498 (2018) 332–340. doi:10.1016/j.jnucmat.2017.10.039.

[18] I. Jolliffe, Principal Component Analysis, Springer Berlin Heidelberg, Berlin, Heidelberg, 2011, pp. 1094–1096. doi:10.1007/978-3-642-04898-455.

[19] Y. Mae, What the DarkenGurry Plot Means About the Solubility of Elements in Metals, Metall and Mat Trans A 47 (12) (2016) 6498–6506. doi:10.1007/s11661-016-3730-1.
URL `https://doi.org/10.1007/s11661-016-3730-1`

[20] J. K.A. Gschneidner, F. Calderwood, The As-Nd (arsenic-neodymium) system, Bull Alloy Phase Diagr 7 (1986) 345–346.

[21] H. Okamoto, As-U (arsenic-uranium), Binary Alloy Phase Diagrams II, Ed., Ed. T.B. Massalski 1 (1990) 330–334.